The University of Texas at El Paso
Department of Mathematical Sciences
Research Reports Series

El Paso, Texas Research Report No. 2007-03

Computer Simulation of a Flow-Thermal Coupled Problem

Pavel Solin, Jakub Cerveny, Lenka Dubcova, Ivo Dolezel

The University of Texas at El Paso
Department of Mathematical Sciences
Research Reports Series

El Paso, Texas Research Report No. 2007-03

Computer Simulation of a Flow-Thermal Coupled Problem

Pavel Solin, Jakub Cerveny, Lenka Dubcova, Ivo Dolezel

The University of Texas at El Paso
Department of Mathematical Sciences

Pavel Solin, Jakub Cerveny, Lenka Dubcova, Ivo Dolezel:
Computer Simulation of a Flow-Thermal Coupled Problem

Abstract: *In this study we apply a higher-order finite element method (hp-FEM) to thermally conductive incompressible fluid flow described by the Navier-Stokes equations. The velocity components* u_1 *and* u_2*, pressure* p*, and temperature* θ *are approximated on four different meshes that are adapted to respect the individual behavior of these physical fields. Such approach leads to a significant reduction of both the size and conditioning of the discrete problem compared to the discretization on a single mesh. The multi-mesh hp-FEM is described and numerical results are presented.*

AMS subject classification: 35B50, 65N60

Keywords: *hp*-FEM, coupled problems, multiple meshes, hanging nodes, automatic adaptivity

Correspondence

solin@utep.edu, jcerveny@utep.edu, ldubcova@utep.edu, doleze@fel.cvut.cz

Acknowledgment

The work of the authors on this project was supported by the Czech Science Foundation Grants No. 102/05/0629 and 102/07/0496 as well as by Grant No. IAA100760702 of the Grant Agency of the Academy of Sciences of the Czech Republic.

The University of Texas at El Paso
Department of Mathematical Sciences
500 West University, El Paso, TX 79968
Email: mathdept@math.utep.edu
URL: http://www.math.utep.edu
Phone: 1.915.747.5761
Fax: 1.915.747.6502

1 Introduction

While numerical methods for single-field problems have reached a high degree of maturity, computational methods for coupled problems have been far less developed. This is, besides other difficulties, due to the following facts:

- Various physical fields such as, e.g., the temperature, velocity, pressure, electric field, or magnetic field exhibit important qualitative differences which make a uniform computational approach to all of them virtually impossible.
- Various physical fields generally belong to different spaces of functions with different conformity requirements.

In order to resolve individual phenomena in various physical fields efficiently, we consider every solution component on an individual mesh with arbitrary-level hanging nodes [3] where, moreover, individual adaptive strategy is employed. At the same time, every physical field is discretized using higher-order finite elements which conform to the correct Sobolev space dictated by the weak formulation. The coupled thermal-flow problem investigated in this study is presented in the next section.

2 Problem Description

Our pilot computations are related to a simplified 2D model of a tankless water heater. In these devices, water is heated at the time of use in contrast to traditional water heaters where hot water is stored in thermally insulated containers. The situation is depicted in Fig. 1.

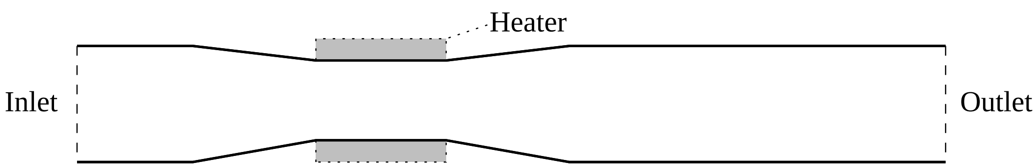

Figure 1: Fluid flow in a heated 2D pipe.

We use the standard incompressible Navier-Stokes equations enhanced with the heat transfer equation for flows, equipped with no-slip boundary conditions on solid walls, prescribed inlet velocity profile, and the standard do-nothing condition at outlet.

Applying the backward Euler method, we obtain a system of PDEs in space formed by the semidiscrete Navier-Stokes equations,

$$
\begin{aligned}
\int \frac{1}{\mathrm{Re}} \nabla u_1^{k+1} \cdot \nabla v_1 \;+ \int (\boldsymbol{u}^k \cdot \nabla)\, u_1^{k+1}\, v_1 + \int \frac{u_1^{k+1}\, v_1}{\tau} - \int p^{k+1} \frac{\partial v_1}{\partial x} &= \int \frac{u_1^k v_1}{\tau}, \\
\int \frac{1}{\mathrm{Re}} \nabla u_2^{k+1} \cdot \nabla v_2 \;+ \int (\boldsymbol{u}^k \cdot \nabla)\, u_2^{k+1}\, v_2 + \int \frac{u_2^{k+1}\, v_2}{\tau} - \int p^{k+1} \frac{\partial v_2}{\partial y} &= \int \frac{u_2^k v_2}{\tau}, \\
\int \frac{\partial u_1^{k+1}}{\partial x} q + \int \frac{\partial u_2^{k+1}}{\partial y} q &= 0,
\end{aligned}
$$

and the heat transfer equation

$$
\lambda \int \nabla \theta^{k+1} \cdot \nabla s \;+ \int (\boldsymbol{u}^k \cdot \nabla)\, \theta^{k+1}\, s + \int \frac{\theta^{k+1}\, s}{\tau} = \int \frac{\theta^k\, s}{\tau} + \beta \int_{\Gamma_N} s.
$$

Here. the symbols $\boldsymbol{u}, p, \theta$ stand for the flow velocity, pressure, and temperature, respectively. Quantities with the superscripts k and $k+1$ correspond to the time levels t^k and t^{k+1}, respectively, and $\tau = t^{k+1} - t^k$ is the time step. The symbols Re, λ, β stand for the Reynolds number, thermal conductivity coefficient of the fluid, and heat flux coefficient of the walls, respectively. The test functions for the velocity components, pressure, and temperature are denoted by v_1, v_2, q, and s respectively. By Γ_N we denote the heated part of the domain boundary which is highlighted by the gray color in Fig. 1.

3 Automatic *hp*-Adaptivity with Arbitrary-Level Hanging Nodes

By automatic *hp*-adaptivity we mean mesh refinement where every element can be either *h*-refined (split in space into smaller elements of the same polynomial degree), *p*-refined (its polynomial degree increased), or split in space with arbitrary polynomial degrees in the element sons (see Fig. 2).

This procedure is profoundly different from standard *h* or *p* adaptivity and it is clear that traditional error estimates (one number per element) are not enough to guide automatic *hp*-adaptivity. The implementation of automatic *hp*-adaptivity is highly nontrivial [1], but it may be simplified by making the element refinements local with the help of arbitrary-level hanging nodes [3].

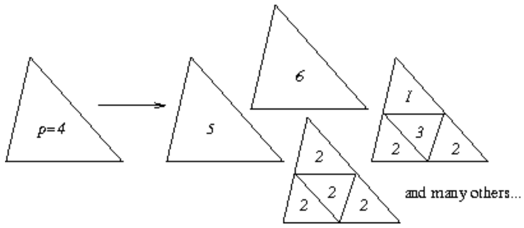

Figure 2: Compared to standard h or p adaptivity, in hp-adaptivity one element can be refined in many different ways.

4 Multi-Mesh Assembling Procedure

The multi-mesh assembling procedure differs from the standard single-mesh case [4] in several aspects. For example, the reference maps are slightly more complicated, and one has to take care about the transfer of data among the meshes. We solve this problem by considering a *united mesh* which is a geometrical union of all meshes (see Fig. 3). This mesh is never created physically, but the element-by-element assembling procedure parses its virtual elements in a similar way as if all fields were discretized on the united mesh.

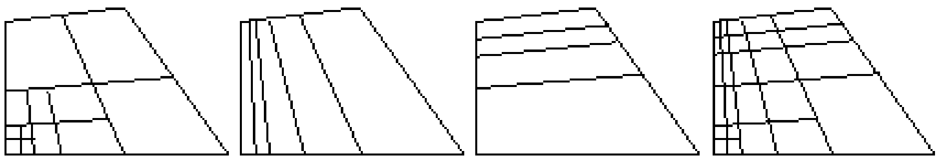

Figure 3: Illustration example of three meshes (left) and the corresponding united mesh (right).

The transfer of functions from all meshes to the united mesh is fully explicit and very fast. Compared to the discretization of all fields on the united mesh, the multi-mesh assembling procedure is slightly slower due to these data transfers. However, it leads to a discrete problem which is smaller and better conditioned. A numerical example is given in the following section.

5 Numerical Example

Let us now return to the model problem introduced in Section 2. Fig. 4 shows the stationary approximations of the velocity components u_1 and u_2, pressure p, and temperature θ. The corresponding Reynolds number is Re = 500. The finite element meshes are shown in Fig. 5.

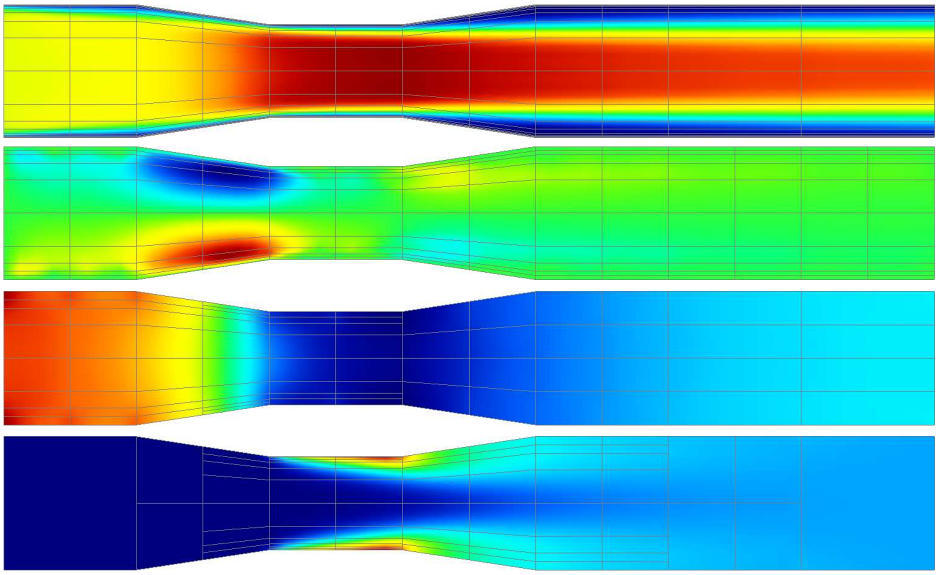

Figure 4: Steady state approximations of u_1, u_2, p, and θ.

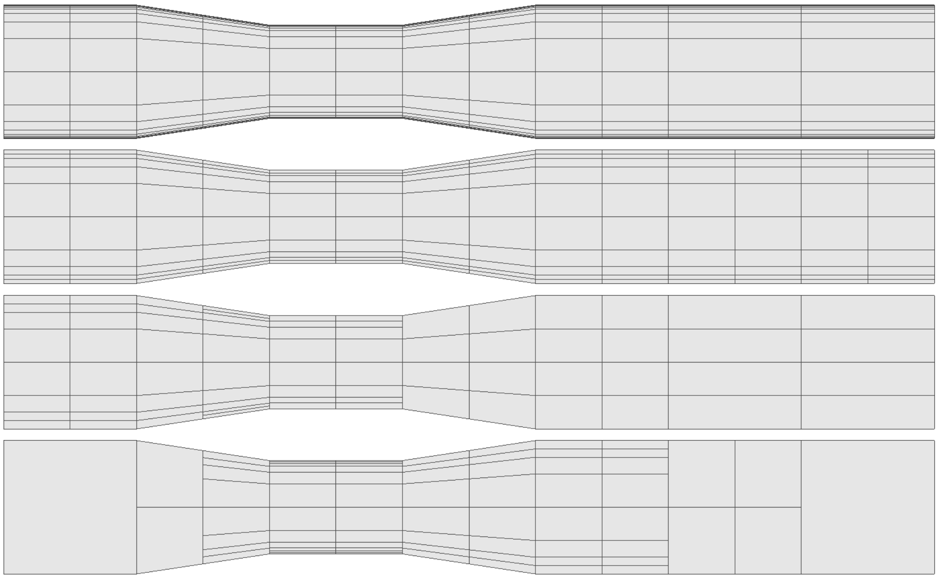

Figure 5: Finite element meshes for u_1, u_2, p, and θ.

Both velocity components u_1, u_2 are approximated using cubic H^1-conforming (continuous) elements. The mesh for the pressure p consists of quadratic L^2-conforming (discontinuous) elements, and the temperature θ is approximated using quadratic H^1-conforming elements. The discrete problem obtained using the multi-mesh assembling procedure has 4443 degrees of freedom (DOF) while the discrete problem on the corresponding united mesh has

7740 DOF. In this case, condition numbers of the two stiffness matrices are too high to be compared numerically. However, when we switch to quadratic H^1-conforming elements for pressure, the numbers of DOF change to 4102 and 6721, and the condition numbers of the corresponding stiffness matrices are 77808 and 835402 (multi-mesh and united mesh, respectively). A full paper about the presented topic including more detailed accuracy, stability, and performance comparisons will appear in near future.

6 Acknowledgment

The work of the authors on this project was supported by the Czech Science Foundation Grants No. 102/05/0629 and 102/07/0496 as well as by Grant No. IAA100760702 of the Grant Agency of the Academy of Sciences of the Czech Republic.

References

[1] L. Demkowicz, W. Rachowicz, and Ph. Devloo. A Fully Automatic hp-Adaptivity. Journal of Scientific Computing 17, Nos 1-3, 127-155 (2002).

[2] P. Šolín. *Partial Differential Equations and the Finite Element Method*, J. Wiley & Sons, 2005.

[3] P. Šolín, J. Červený, I. Doležel. Arbitrary-Level Hanging Nodes and Automatic Adaptivity in the hp-FEM, Math. Comp. Sim., accepted (2006).

[4] P. Šolín, K. Segeth, I. Doležel. *Higher-Order Finite Element Methods*, Chapman & Hall/CRC Press, Boca Raton (2003).

[5] P. Šolín, T. Vejchodský. Continuous *hp* Finite Elements Based on Generalized Eigenfunctions. Research Report No. 2006-08, Department of Mathematical Sciences, University of Texas at El Paso (2006).

[6] P. Šolín, T. Vejchodský. Higher-Order Finite Elements Based on Generalized Eigenfunctions of the Laplacian, submitted, August 2006.